Cosserat elasticity of negative Poisson's ratio foam: experiment

Zach Rueger and Roderic S. Lakes*

August 16, 2016

Department of Engineering Physics, Department of Materials Science
University of Wisconsin, Madison, WI 53706-1687, USA
Keywords (negative Poisson's ratio, auxetic, Cosserat)
* Corresponding author. email lakes@engr.wisc.edu Phone: +00 608 265 8697

preprint adapted from Rueger, Z. and Lakes, R. S., Cosserat elasticity of negative Poisson's ratio foam: experiment, Smart Materials and Structures, 25 054004 (8pp) (2016).

Abstract

Negative Poisson's ratio polymer foams derived from reticulated open cell foams exhibit large size effects in torsion and bending. Effective moduli increase as diameter decreases in contrast to the prediction of classical elasticity. Size effects of this sort are predicted by Cosserat (micropolar) elasticity in which points can rotate as well as translate and distributed moments are incorporated. The Cosserat coupling number N was about twice as large as that of as-received foam, leading to strong effects. The torsion characteristic length ℓ_t was similar. Cosserat effects are known to enhance toughness and immunity from stress concentration.

1 Introduction

All physical materials have microstructure, but for many practical purposes it is helpful to represent them as continuous media. Continuum theories with different amounts of freedom are available. An early theory of Navier [1] was called uniconstant elasticity and was based on a theory that assumed atomic interactions entailed central forces and affine motion of atoms. It allows only one isotropic elastic constant, a modulus. It was abandoned since it predicted a Poisson's ratio of 1/4 for all isotropic materials; early experiments showed many common materials to have Poisson's ratio between 0.3 and 0.4. The elasticity theory currently accepted as classical allows Poisson's ratios in isotropic materials in the range -1 to $1/2$; there are two independent isotropic elastic constants. The accepted range for Poisson's ratio in isotropic solids was commonly taken as 0 to 1/2 based on experience with common materials, though some anisotropic single crystals with negative Poisson's ratio were known as well as negative Poisson's ratio in a model of rods, hinges and springs [2]. In 1987 a 3D negative Poisson's ratio material based on transformed open cell polyurethane foam was reported [3]; it had a Poisson's ratio of -0.7. The manufacturing process described in this Science article stimulated much continuing research in the field of designed materials. The negative Poisson's ratio in foams depends on cell structure rather than chemistry; indeed, metallic and thermoset polymer foams have been prepared with negative Poisson's ratio [4]. Negative Poisson's ratio was also designed in 2D systems with rotating hexamers [5] [6]; thermodynamic stability was analyzed. Void space is not required to achieve a negative Poisson's ratio; a hierarchical two phase composite [7] can approach the lower limit -1 provided there is sufficient contrast between

constituent properties. Negative Poisson's ratio, also called auxetic in a 1991 article proposing molecular scale design, was analyzed in foams [8]. Negative Poisson's ratio can be achieved in other 2D structures containing rotating rigid units such as squares [9]. In all these examples, the material has been considered to be classically elastic. Initial evidence of non-classical characteristics was revealed by holography in non-affine heterogeneous deformation of conventional and negative Poisson's ratio copper foams [10] and in size effects in negative Poisson's ratio polymer foam [11].

Classical elasticity has no length scale. By contrast, Cosserat elasticity [12] [13], also called micropolar elasticity [14], allows rotations of points and has a length scale, so it is pertinent to the deformation of heterogeneous materials in which the heterogeneity size scale cannot be neglected in comparison to dimensions of a structural component or of structural heterogeneities such as holes or cracks. Soon after the initial article on negative Poisson's ratio foam, it was suggested that the effect was due to the coarse cell structure and Cosserat effects in the associated continuum view. However Poisson's ratio is a classical concept; moreover the range of Poisson's ratio for Cosserat solids is the same as the range for classical ones: -1 to $1/2$. Too, the simple tension experiment used to reveal Poisson's ratio has no associated length scale and does not excite the rotational degrees of freedom required to produce non-classical effects in a Cosserat elastic material [15]. Foams and honeycombs, though they can have substantial cell sizes, are commonly treated as classical continua [17]. Only toughness of foams is related to the size scale of the cells [17]; the treatment is nonetheless classical. Cosserat elastic solids, if isotropic, have six elastic constants. Deviations from classical elasticity have long been known. For example, Brillouin [18] studied wave propagation in crystal lattices; a spring mass model discloses dispersion of waves, in harmony with experimental observations of high frequency ultrasonic waves in crystals. Dispersion and cut off frequency effects can be modeled from a continuum perspective. For example, the microstructure elasticity theory of Mindlin [19], allows points in the continuum to translate, rotate, and deform. Such a theory, also called micromorphic, is more complex than classical or Cosserat elasticity; for an isotropic solid, there are 18 micromorphic elastic constants compared with 6 for Cosserat elasticity and 2 for classical elasticity. The allowable range of Poisson's ratio in microstructure elasticity is not stated directly. However, energy based limits for tensorial constants in microstructure elasticity imply a range of Poisson's ratio equivalent to that in classical elasticity. Microstretch elasticity is also a subset of microstructure / micromorphic elasticity, one that incorporates the Cosserat type freedom as well as sensitivity to dilatation gradient [20]. There are 9 isotropic elastic constants. As with microstructure elasticity, allowable range of Poisson's ratio in is not stated directly. However, energy based limits for tensorial constants suggest a range of Poisson's ratio equivalent to that in classical elasticity.

The physical origin [21] of the Cosserat couple stress in cellular solids is the summation of bending and twisting moments transmitted by ribs in a foam or by structural elements in other materials (Figure 1). The local rotation in the Cosserat continuum corresponds to the rotation of ribs. Forces and moments are also considered in the classic analyses of foam by Gibson and Ashby [17] in which classical elastic moduli were determined; effects of rotation gradients were not considered.

The Cosserat theory of elasticity is a continuum theory that incorporates a specific kind of nonlocal [22] interaction. The stress σ_{jk} (force per unit area) can be asymmetric. The moment arising from this asymmetry is balanced by a couple stress m_{jk} (a torque per unit area). The antisymmetric part of the stress is related to local rotations. $\sigma_{jk}^{antisym} = \kappa e_{jkm}(r_m - \phi_m)$ in which κ is an elastic constant, ϕ_m is the rotation of points, called micro-rotation, e_{jkm} is the permutation symbol, and $r_k = \frac{1}{2} e_{klm} u_{m,l}$ is the "macro" rotation based on the antisymmetric part of gradient of displacement u_i. The constitutive equations [14] for linear isotropic Cosserat elasticity are as

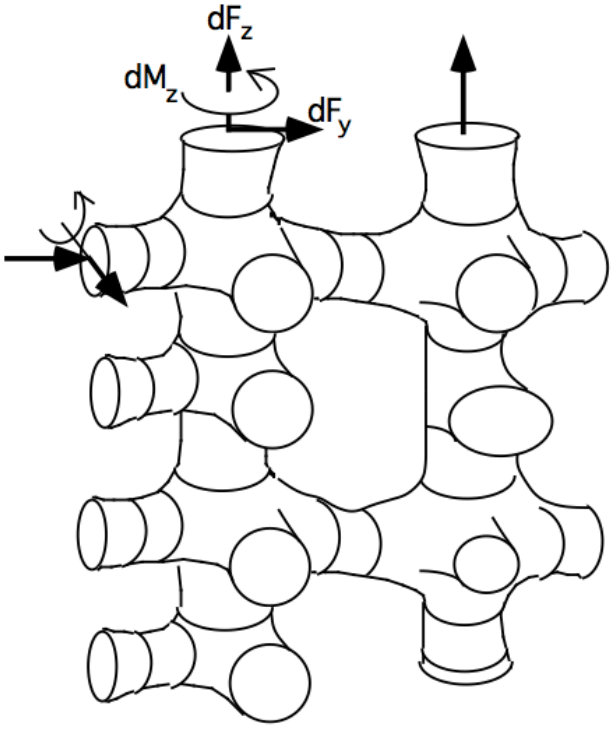

Figure 1: Ribs of foam or lattice with increment of force dF and increment of moment dM.

follows.

$$\sigma_{ij} = 2G\epsilon_{ij} + \lambda\epsilon_{kk}\delta_{ij} + \kappa e_{ijk}(r_k - \phi_k) \tag{1}$$

$$m_{ij} = \alpha\phi_{k,k}\delta_{ij} + \beta\phi_{i,j} + \gamma\phi_{j,i} \tag{2}$$

Cosserat elasticity allows sensitivity to gradients of rotation because rotations and stresses are coupled. One may also formulate a generalized continuum theory with sensitivity to gradients of dilatation [23] rather than rotation.

There are six independent isotropic Cosserat elastic constants λ, G, α, β, γ, κ. The following technical constants, beneficial for physical insight, are obtained from them. As in classical elasticity, several are interrelated; specifically of the seven below, the classical relation between E, G and ν applies. Here λ is a Lamé constant from elasticity theory.

$$Young's\ modulus \qquad E = \frac{G(3\lambda + 2G)}{\lambda + G} \tag{3}$$

$$Shear\ modulus \qquad G \tag{4}$$

$$Poisson's\ ratio \qquad \nu = \frac{\lambda}{2(\lambda + G)} \tag{5}$$

$$Characteristic\ length,\ torsion \qquad \ell_t = \sqrt{\frac{\beta + \gamma}{2G}} \tag{6}$$

$$Characteristic\ length,\ bending \qquad \ell_b = \sqrt{\frac{\gamma}{4G}} \tag{7}$$

$$Coupling\ number \qquad N = \sqrt{\frac{\kappa}{2G + \kappa}} \tag{8}$$

$$Polar\ ratio \qquad \Psi = \frac{\beta + \gamma}{\alpha + \beta + \gamma}. \tag{9}$$

Predictions of Cosserat elasticity differ from those of classical elasticity. A size effect is predicted in the torsion [24] and bending [25] of circular cylinders of Cosserat elastic materials. Thin cylinders appear more stiff than expected classically. A size effect is also predicted in the bending of plates [24] . In tension or compression there is no size effect. The stress concentration factor for a circular hole is smaller than the classical value; small holes exhibit less stress concentration than larger ones [26].In classical elastic solids, by contrast, there is no size effect in torsion or bending; structural rigidity goes as the fourth power of the radius; stress concentration is independent of hole size.

Cosserat elastic effects have been observed experimentally in several materials with microstructure. Size effects which occur in torsion and bending of closed cell foams [27], [28] and of compact bone [29] are consistent with Cosserat elasticity. The apparent modulus increases substantially as the specimen diameter becomes smaller. This observation is in contrast to the predictions of classical elasticity. Cosserat elasticity can account for these observations. Dense (340 kg/m^3) closed cell polyurethane foam [27] has elastic constants $E = 300$ MPa, $G = 104$ MPa, $\nu = 0.4$, $\ell_t = 0.62$ mm, $\ell_b = 0.33$ mm, $N^2 = 0.04$, $\Psi = 1.5$. The cell size is from 0.05 mm to 0.15 mm. For dense (380 kg/m^3) polymethacrylamide closed cell foam (Rohacell WF300) [28], $E = 637$ MPa, $G = 285$ MPa, $\ell_t = 0.8$ mm, $\ell_b = 0.77$ mm, $N^2 \approx 0.04$, $\Psi = 1.5$. The cell size is about 0.65 mm.

The Cosserat characteristic length was determined for a two dimensional polymer honeycomb [30]. Warp of a bar of rectangular cross section in torsion is predicted to be reduced in a Cosserat elastic solid [31]. Such non-classical warp was observed in compact bone [32]. Deformation spills over into the corner region where it would be zero in classical elasticity [33] as revealed by holography. This ameliorates concentration of strain. Strain at the corner entails asymmetry of the stress as predicted by Cosserat elasticity. The reduction of warp deformation has been observed via holography [34]. Cosserat effects were also observed in open cell polymer foam [35].

The present research deals with experimental study of size effects and Cosserat elasticity in negative Poisson's ratio foams derived from low density open cell polymer foams.

2 Methods

2.1 Materials and experiment

Negative Poisson's ratio foam (Figure 3) based on reticulated polyurethane foam (Scott Industrial foam [16]) was used. The as-received foam had average cell size 1.2 mm or 20 pores per inch.

The initial density was 30 kg/m^3. The foam was converted to negative Poisson's ratio foam via triaxial compression and heat treatment [3]. The density calculated for the foam was 96 kg/m^3 corresponding to a volumetric compression ratio of 3.2.

Cylinders were cut from polymer foam with a hot wire cutter such that the cylinder diameter and length were equal. The wire was Nichrome heater wire of thickness 0.015 inches and resistance 2.5 Ω. The electric current was 3 Amps. The initial cylinder cut from the foam was approximately 22 mm in both diameter and length. The foam cylinder was weighed with an analytical balance. Circular end pieces the same diameter as the foam sample were cut from heavy card stock and cemented to both bases of the cylindrical specimen using cyanoacrylate (Loctite 401) over the entire surface. A catalyst was applied to the surfaces being cemented to minimize the amount of cement used and prevent ingression of the cement into the pores of the foam. Slight pressure was applied to the end pieces to ensure good adhesion.

These specimens were tested for torsional and bending rigidity using a Broadband Viscoelastic Spectrometer (BVS) [36] [37]. This instrument uses a Helmholtz coil which acts upon a magnet attached to the specimen to generate torque. The coil spacing is smaller than the larger specimens so a short stalk with a magnet and mirror on the end was fixed to one of the end pieces. A thin aluminum end layer was also cemented to provide a sufficiently rigid attachment for the stalk. A small mirror was first glued to one face of a cubic magnet. The magnet was then calibrated using the BVS and a lock-in amplifier. The magnetic calibration constants of this magnet were obtained by testing a 6061 aluminum alloy rod of known elastic properties. The calibration constants were 8.00 $\times 10^{-6}$ Nm/A in torsion and 1.84 $\times 10^{-5}$ Nm/A in bending. The free end piece of the polymer foam cylinder was cemented to a steel adapter which was screwed in to a 25 mm thick steel rod to support the specimen inside the BVS. Viscoelastic strain was allowed to recover overnight prior to testing to enable stable measurements. The specimen was lowered into the BVS such that the magnet was centered in the Helmholtz coils of the BVS. The lower limit on specimen size was imposed by obtrusive presence of incomplete cells; also by difficulty in handling. A typical specimen of this foam is shown in Figure 2.

Deformation was measured via a beam from a semiconductor laser reflected from a mirror attached to the magnet on the specimen free end. The laser beam was reflected onto a silicon light detector.The laser based displacement sensor was calibrated prior to testing. This was done by first centering the beam upon the detector. The light detector was moved a known amount via a calibrated stage. A calibration curve was obtained via micrometer adjustment. The change in output voltage per change in position was used as the beam position calibration constant (in V/μm).

A sinusoidal signal with a frequency of 1 Hz from a function generator (SRS Model DS345) was input to the torsion Helmholtz coil to test the sample. Because the same frequency was used for all specimen diameters, viscoelastic effects are decoupled from the size effects to be studied. The torque signal was obtained as the voltage across a resistor in series with the coil to eliminate effects of inductive reactance from the coil. The 1 Hz frequency was well below any resonant frequencies. The torque signal vs. angular displacement signal was displayed on a digital oscilloscope (Tektronix TDS3014B) using DC coupling as a Lissajous figure, and used to calculate the modulus and viscoelastic damping of the material.

For bending, the light detector mode was switched to vertical detection and the beam calibration constant was determined accordingly. The driving signal to generate torque was input to the orthogonal bending Helmholtz coil. A correction was applied to account for the additional bending moment imposed by the weight of the magnet and stalk; this correction was 4% or less.

Compression tests were done to ascertain the behavior of the foam in the absence of macroscopic gradients of strain and rotation. This was done by gluing one end piece to a base anchored to an

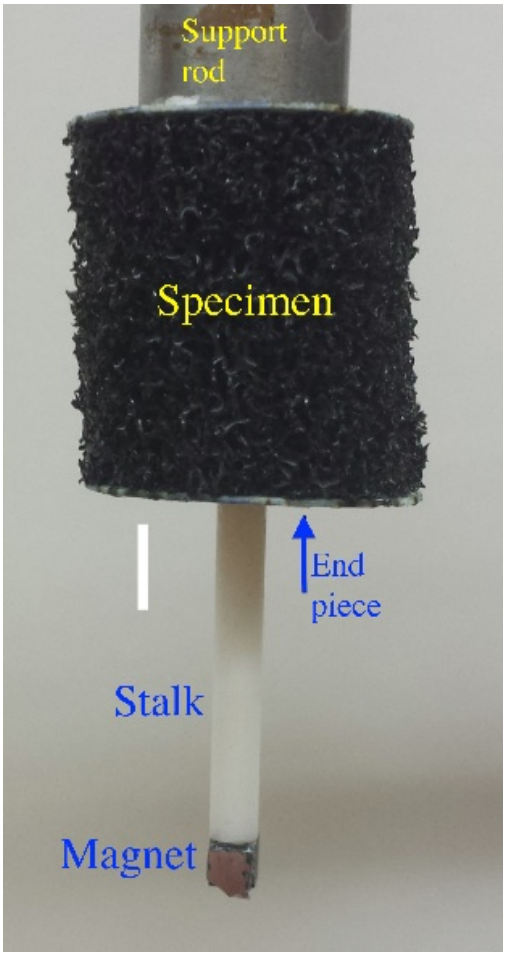

Figure 2: A specimen of foam with attached stalk and magnet. White scale bar: 5mm.

optical table. Force was applied via dead weights placed on the top end piece. Deformation was measured using a linear variable differential transformer (LVDT); its stem was cemented to the top end piece. The LVDT was calibrated using a micrometer driven translation stage. The maximum strain achieved was 4.4%, well within the linear range for a flexible foam. A lower limit on specimen size was imposed by the tendency of small specimens to buckle.

After all testing was completed on a sample it was cut to a smaller length and diameter and the same series of tests were conducted. This process was repeated for a total of ten sample sizes down to a diameter of 3.4 mm. The lower limit on specimen size was imposed by incomplete cells and difficulty in handling.

2.2 Analysis and interpretation

Size effect results were interpreted using available exact analytical solutions for torsion and bending of a Cosserat elastic solid. The shear modulus G was found from the asymptote of torsion rigidity vs. diameter curve for large size. The torsion characteristic length ℓ_t was found from fitting the points for the larger specimens to an approximate solution that is asymptotically valid for large size. A Cosserat elastic circular rod of radius r exhibits the following ratio of structural rigidity to

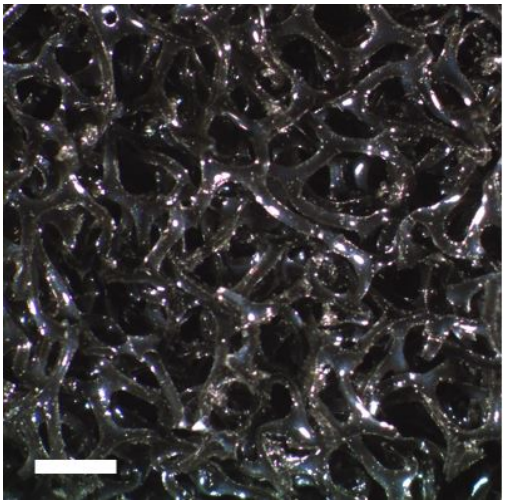

Figure 3: Structure of negative Poisson's ratio foam. Reflected light micrograph. Scale bar: 1 mm.

its classical counterpart (in the absence of gradient, for large diameter).

$$\Omega \approx 1 + 6(\ell_t/r)^2. \tag{10}$$

Size effects occur in torsion: slender specimens appear to have a higher effective modulus than thick ones. The classical torsional rigidity is $\frac{M}{\theta} = G[\frac{\pi}{2}r^4]$. For Cosserat elasticity in this regime, $\frac{M}{\theta} = G[\frac{\pi}{2}r^4](1 + 6(\ell_t/r)^2)$. G is the true shear modulus in the absence of gradients; M is applied moment and θ is angular displacement. This expression is exact for $N = 1$; for other N the exact solution involves Bessel functions [24]:

$$\Omega = (1 + 6(\ell_t/r)^2)[\frac{(1 - 4\Psi\chi/3)}{1 - \Psi\chi}], \tag{11}$$

in which $\chi = I_1(pr)/prI_0(pr)$, $p^2 = 2\kappa/(\alpha + \beta + \gamma)$ and I_0 and I_1 are modified Bessel functions of the first kind.

The shear modulus G and characteristic length ℓ_t were determined by fitting experimental data for the three largest specimens to Eq. 10. The value of N was found by fitting Eq. 11 to the full data set using MATLAB. The constant Ψ only has an appreciable influence for very small radius specimens.

For bending, the classical bending rigidity is $\frac{M}{\theta} = E[\frac{\pi}{4}r^4]$. For bending of a Cosserat elastic circular rod and radius r, the rigidity ratio for small characteristic length $\ell_b << r$ is

$$\Omega \approx 1 + 8(\ell_b/r)^2 \frac{(1 - (\beta/\gamma)^2)}{(1 + \nu)}. \tag{12}$$

This expression is exact if $\beta/\gamma = -\nu$. The Young's modulus E and an initial value for the characteristic length ℓ_b were determined by fitting data for the three largest specimens to Eq. 12, with N input from the torsion analysis, and an initial value $\beta/\gamma = 0.8$ based on prior experimental results on other foams and ν from prior experimental results on negative Poisson's ratio foams.

Finally the values of ℓ_b and β/γ were found by fitting the bending exact solution [25] Eq. 13 to the full data set using MATLAB.

$$\Omega = 1 + 8(\ell_b/r)^2 \frac{(1-(\beta/\gamma)^2)}{(1+\nu)} + \frac{8N^2}{(1+\nu)}[\frac{(\beta/\gamma+\nu)^2}{\zeta(\delta a)+8N^2(1-\nu)}] \quad (13)$$

with $\delta = N/\ell_b$ and $\zeta(\delta r) = (\delta r)^2[((\delta r)I_0((\delta r)) - I_1((\delta r)))/((\delta r)I_0(\delta r) - 2I_1(\delta r))]$.

3 Results and discussion

Density of foam specimens was 96 kg/m^3 and was independent of specimen diameter to within a few percent. As for tests of anisotropy, the as-received foam was anisotropic [35], with a ratio of compressive moduli in different directions of 1.6.

Results of torsion size effect studies are shown in Figure 4.

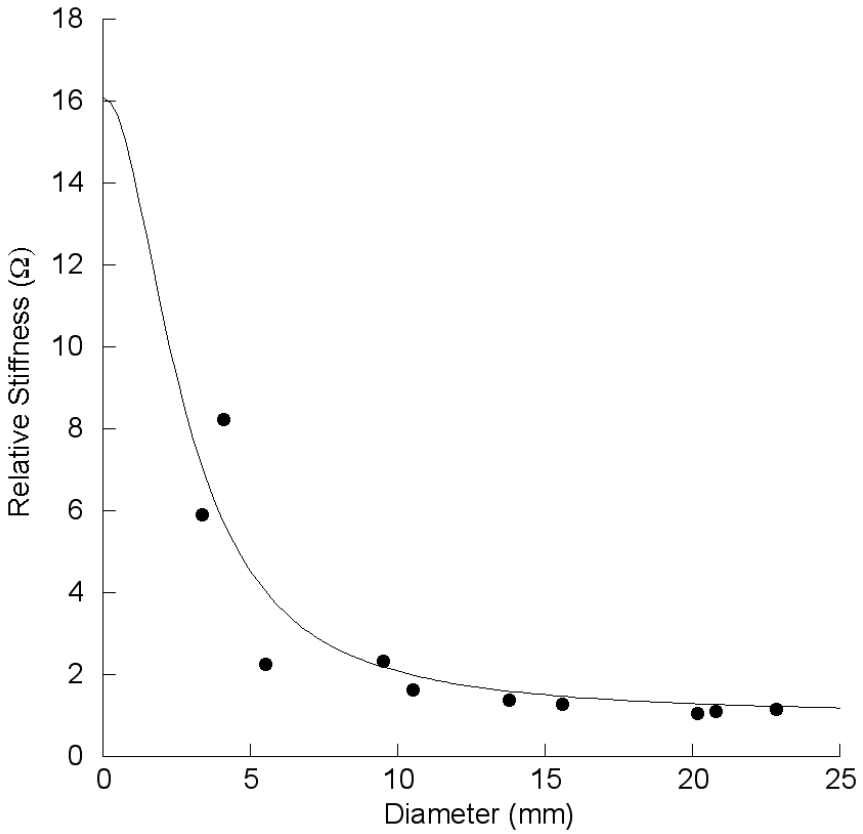

Figure 4: Size effects for negative Poisson's ratio foam in torsion. Points are experimental. Curve is theoretical for $G = 16$ kPa, $\ell_t = 2.3$ mm $N = 0.78$ and $\Psi = 1.5$. Classical elasticity predicts constant $\Omega = 1$ independent of diameter.

For negative Poisson's ratio foam, $G = 16$ kPa, $\ell_t = 2.3$ mm $N = 0.78$ and $\Psi = 1.5$.

By contrast, the as-received foam [35] had $G = 45$ kPa and the characteristic length for torsion was $\ell_t = 2.1$ mm. Moreover $N = 0.41$, and $\Psi = 1.5$. So the negative Poisson's ratio foam had N about twice as large as that of as-received foam and ℓ_t was similar. The goodness of fit was $R^2 = 0.79$. The maximum size effect in torsion for as-received foam was $\Omega = 2.2$. The larger maximum

size effect, about 8 in negative Poisson's ratio foam, is associated with the larger coupling number N.

The compression tests disclosed $E = 25$ kPa with no consistent dependence on diameter. Results of bending size effect studies are shown in Figure 5. Assuming $E = 25$ kPa based on compression and $N = 0.78$ based on torsion, the best fit for the remaining constants for negative Poisson's ratio foam was $\ell_b = 3.9$ mm, $\beta/\gamma = 0.8$, with goodness of fit $R^2 = 0.81$. If however one ignores the compression result and conducts a fit, the result is $E = 38$ kPa, $\ell_b = 3.0$ mm, $\beta/\gamma = 0.87$, with goodness of fit $R^2 = 0.81$. Also, the asymptote for large size in the bending studies would be better delineated if larger specimens were available, however the processing used to obtain negative Poisson's ratio foam resulted in rectangular bars about 25 mm in square cross section. The bars as received foam were about twice as wide, and were cut to appropriate width to obtain the correct volumetric compression. For this material, bending of the largest specimens resulted in a better value of E. The range of values that are tolerable to the fitting process is attributed to the scatter in the data points and to the accessible range in specimen diameter. As for the range in ℓ_b for bending, values between about 3 mm to 4.7 mm gave $R^2 > 0.6$ in contrast to $R^2 = 0.81$ for the best fit $\ell_b = 3.9$ mm. As for the range of N, values between 0.62 and 9 gave $R^2 > 0.6$ in contrast to $R^2 = 0.81$ for the best fit $N = 0.78$.

By contrast, the as-received foam [35] had $E = 91$ kPa, $\ell_b = 9$ mm, $\beta/\gamma = 0.83$; $N = 0.41$. The maximum size effect for as-received foam in bending was $\Omega = 3$. As with torsion, the negative Poisson's ratio foam exhibited a much larger size effect ratio $\Omega = 18$, attributed to the larger N.

The Poisson's ratio of the as-received foam was determined [38] to be approximately 0.3. This value was also given by [17] as the mean of measurements by various authors on different foams of conventional structure. The Poisson's ratio of the negative Poisson's ratio foam was inferred to be -0.63 based on the initial and final density [39]. Specimens were sufficiently short that direct measurement of Poisson's ratio was not practical. Nevertheless, stretching of thin slices revealed the Poisson's ratio to be negative. The relationship between moduli and Poisson's ratio implies anisotropy. That is not surprising in view of the modest anisotropy of the as received foam. It is possible to make fully isotropic negative Poisson's ratio foam [40] via further effort in processing.

It is of interest to compare the inferred characteristic lengths with the foam cell size. The as-received foam had an average cell size of 1.2 mm. Volumetric compression by a factor of 3.2 to produce the negative Poisson's ratio foam reduces the cell size and also causes the folded-in re-entrant structure that gives rise to the negative Poisson's ratio. The effective cell size may be taken as 1.2 mm / $3.2^{1/3} = 0.81$ mm. Both characteristic lengths are considerably larger than this, a fact attributed to the bend dominated role of the foam ribs.

As for other foams as Cosserat solids, experiments on dense closed cell foams [27], [28] revealed a relatively small $N = 0.2$, so size effects were comparatively weak. The maximum size effect ratio was $\Omega = 1.3$ for dense polyurethane foam and 1.44 for closed cell Rohacell foam, much smaller than in the present foams. Foam [28] with relatively uniform cell size had ℓ comparable to the cell size. Foam [27] heterogeneous in its cell size had ℓ larger than the cell size. The structures, as well as the structure of the as received foam, differ considerably from that of the negative Poisson's ratio re-entrant foams examined here.

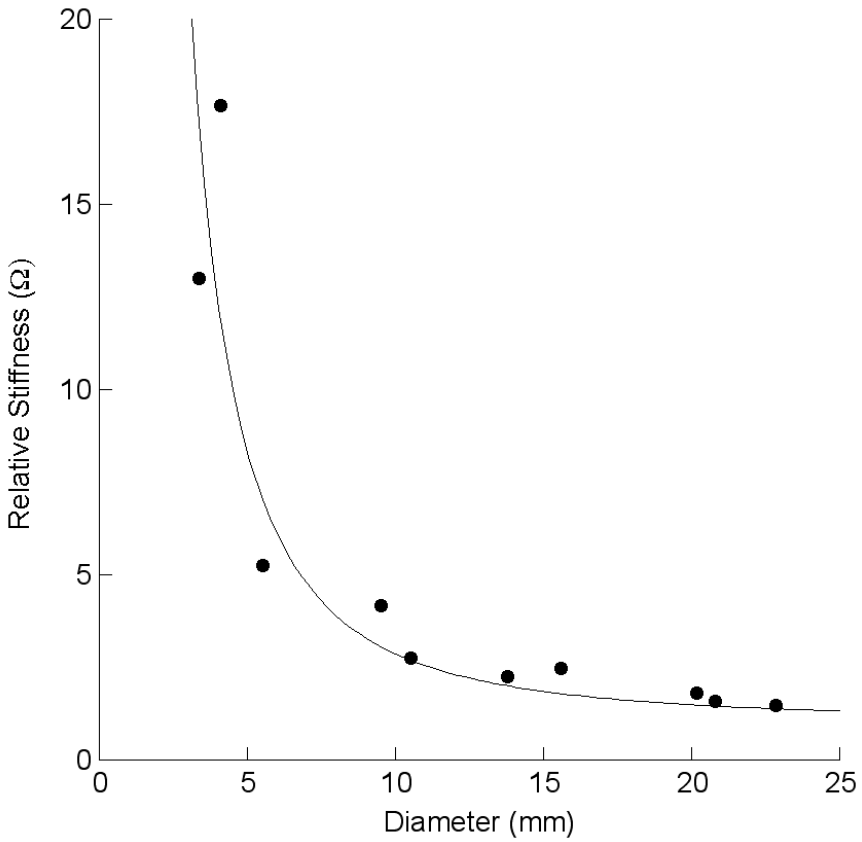

Figure 5: Size effects for negative Poisson's ratio foam in bending. Points are experimental. Curve is theoretical for $E = 25$ kPa $N = 0.78$, $\ell_b = 3.9$ mm, and $\beta/\gamma = 0.88$. Classical elasticity predicts constant $\Omega = 1$ independent of diameter.

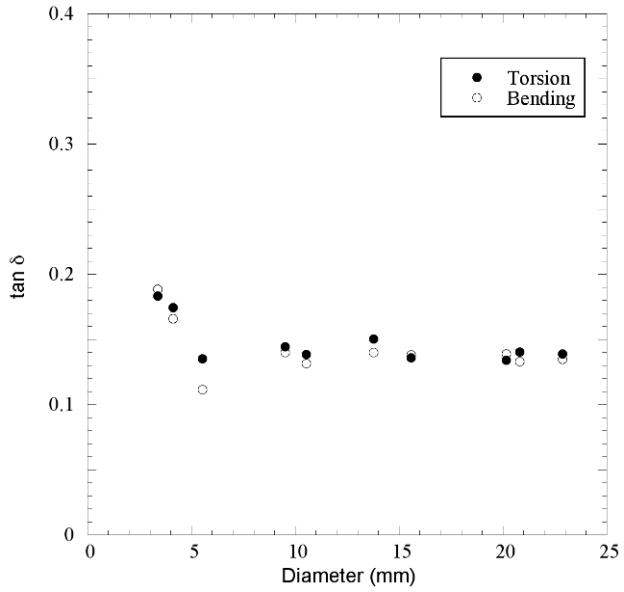

Figure 6: Viscoelastic tan δ vs. specimen size for negative Poisson's ratio foam. Open circles: bending. Solid circles: torsion.

Damping tan δ of the foam was essentially independent of specimen size, as shown in Figure 6 but the two smallest sizes showed a somewhat higher damping. tan δ was similar to that of as-received foam suggesting no obvious change in cross link density or other molecular aspects as a result of the processing used to obtain negative Poisson's ratio foam. By contrast, a dependence of modulus and damping on processing [41] was observed in which damping increased statistically with permanent compression hence with the reduction in Poisson's ratio. Both these polyurethane foams were prepared via triaxial compression followed by heat treatment [3]. One can also prepare auxetic foam and revert it to a positive Poisson's ratio via a solvent treatment [42]. The influence of processing procedure on structure and properties has been analyzed [43].

Scatter in the data points is attributed to incomplete cells at the specimen surface, also to larger scale heterogeneity in the foam. Similar scatter was observed in the as-received foam.

As for comparison with theory, no known analysis is available for the structure of the present foam. Cosserat elastic constants have been calculated from theoretical homogenization of several lattices with straight ribs [44] [45] [46]. These are stretch dominated so the effects of rib bending and torsion are much smaller than the effects of rib extension. The characteristic lengths of such lattices are much smaller than the cell size. Two dimensional chiral honeycomb lattice structures analyzed as Cosserat continua disclosed bend dominated behavior in which Young's modulus is governed by rib bending. These honeycombs have large N approaching its upper bound 1, and characteristic length ℓ comparable to the cell size [47]. Sigmoid curvature of the lateral surfaces of bent square cross section bars was analyzed via Cosserat elasticity [48]. Such curvature requires $\beta/\gamma \neq -\nu$ and indeed it was observed in conventional as-received open cell foam. Although no formal measurements were made with the negative Poisson's ratio foam (for which $\beta/\gamma \approx -\nu$), visual observation of such bending of a square cross section bar suggested any sigmoid curvature must be small.

In summary, large size effects are observed in the torsion of negative Poisson's ratio open cell foam. The effects are consistent with Cosserat elasticity. Results do not necessarily exclude the

presence of additional freedom such as that incorporated in micromorphic / Mindlin microstructure [19] theory or in microstretch elasticity [20].

4 Conclusions

Large size effects were observed in the torsion and bending of negative Poisson's ratio open cell polymer foams. These effects are inconsistent with classical elasticity but can be modeled with Cosserat elasticity. The negative Poisson's ratio foam had Cosserat coupling number N about twice as large as that of as-received foam; torsion characteristic length ℓ_t was similar, and bending characteristic length ℓ_b was smaller. Maximum size effects were larger than those in as-received foam. This is attributed to the larger N. Cosserat solids are known to exhibit enhancement in toughness and immunity from stress concentrations, a beneficial characteristic.

5 Acknowledgements

We gratefully acknowledge support of this research by the National Science Foundation via Grant CMMI-1361832.

References

[1] S. P. Timoshenko, History of Strength of Materials, Dover, NY, (1983).

[2] R. F. Almgren, An isotropic three dimensional structure with Poisson's ratio = - 1, Journal of Elasticity; **15** (4): 427-30 (1985).

[3] R. S. Lakes, Foam structures with a negative Poisson's ratio, Science, **235** 1038-1040 (1987).

[4] E. A. Friis, R. S. Lakes, and J. B. Park, Negative Poisson's ratio polymeric and metallic materials, Journal of Materials Science, **23**, 4406-4414 (1988).

[5] K. W. Wojciechowski, Constant thermodynamic tension Monte Carlo studies of elastic properties of a two-dimensional systems of hard cyclic hexamers, Molecular Physics **61**, 1247-125 (1987).

[6] K. W. Wojciechowski, Two-dimensional isotropic system with a negative Poisson ratio. Physics Letters A, **137**, 60-64, (1989).

[7] G. Milton, Composite materials with Poisson's ratios close to -1. J. Mech. Phys. Solids, **40**: 1105-1137 (1992).

[8] K. E. Evans, M.A. Nkansah, I. J. Hutchinson, Auxetic foams - modeling negative Poisson's ratios, Acta Metall Mater **42** (4): 1289-1294 (1994).

[9] J. N. Grima, A. Alderson, K. E. Evans, Auxetic behaviour from rotating rigid units. Physica Status Solidi B, **242**, 561-75 (2005).

[10] C. P. Chen and R. S. Lakes, Holographic study of conventional and negative Poisson's ratio metallic foams: elasticity, yield, and micro-deformation, J. Materials Science, **26**, 5397-5402 (1991).

[11] R. S. Lakes, Experimental micro mechanics methods for conventional and negative Poisson's ratio cellular solids as Cosserat continua, J. Engineering Materials and Technology, **113**, 148-155 (1991).

[12] E. Cosserat, and F. Cosserat, *Theorie des Corps Deformables*, Hermann et Fils, Paris (1909).

[13] R. D. Mindlin, Stress functions for a Cosserat continuum, Int. J. Solids Structures, **1**, 265-271 (1965).

[14] A. C. Eringen, Theory of micropolar elasticity. In *Fracture*, 1, 621-729 (edited by H. Liebowitz), Academic Press, NY (1968).

[15] R. S. Lakes, Negative Poisson's ratio materials, Science, **238** 551 (1987).

[16] Foamade Industries, Auburn Hills, MI.

[17] L. J. Gibson, M. F. Ashby, G. S. Schajer, and C. I. Robertson, The mechanics of two dimensional cellular solids, Proc. Royal Society London, **A382**, 25-42 (1982).

[18] L. Brillouin, *Wave Propagation in Periodic Structures*, Dover, N.Y. (1953)

[19] R. D. Mindlin, Micro-structure in linear elasticity, Arch. Rational Mech. Analy, **16**, 51-78, (1964).

[20] A. C. Eringen, Theory of thermo-microstretch elastic solids, Int. J. Engng. Sci., **28** (12) 1291-1301, (1990).

[21] R. S. Lakes, Experimental methods for study of Cosserat elastic solids and other generalized continua, in Continuum models for materials with micro-structure, ed. H. Muhlhaus, J. Wiley, N. Y. Ch. 1, p. 1-22, (1995).

[22] L. Ilcewicz, T. C. Kennedy and C. Shaar, Experimental application of a generalized continuum model to nondestructive testing, J. Materials Science Letters **4**, 434-438 (1985).

[23] S. C. Cowin and J. W. Nunziato, Linear elastic materials with voids, J. Elasticity **13** 125-147 (1983)

[24] R. D. Gauthier and W. E. Jahsman, A quest for micropolar elastic constants. J. Applied Mechanics, **42**, 369-374 (1975).

[25] G. V. Krishna Reddy and N. K. Venkatasubramanian, On the flexural rigidity of a micropolar elastic circular cylinder, J. Applied Mechanics **45**, 429-431 (1978).

[26] R. D. Mindlin, Effect of couple stresses on stress concentrations, Experimental Mechanics, **3**, 1-7, (1963).

[27] R. S. Lakes, Experimental microelasticity of two porous solids, Int. J. Solids and Structures, **22**, 55-63 (1986).

[28] W. B. Anderson and R. S. Lakes, Size effects due to Cosserat elasticity and surface damage in closed-cell polymethacrylimide foam, J. Materials Science, **29**, 6413-6419 (1994).

[29] R. S. Lakes, On the torsional properties of single osteons, J. Biomechanics, **28**, 1409-1410 (1995).

[30] R. Mora and A. M. Waas, Measurement of the Cosserat constant of circular cell polycarbonate honeycomb, Philosophical Magazine A, **80**, 1699-1713 (2000).

[31] H. C. Park and R. S. Lakes, Torsion of a micropolar elastic prism of square cross section. Int. J. Solids, Structures, **23**, 485-503 (1987).

[32] H. C. Park and R. S. Lakes, Cosserat micromechanics of human bone: strain redistribution by a hydration-sensitive constituent, J. Biomechanics, **19**, 385-397 (1986).

[33] R. S. Lakes, D. Gorman, and W. Bonfield, Holographic screening method for microelastic solids, J. Materials Science, **20**, 2882-2888 (1985).

[34] W. B. Anderson, R. S. Lakes, and M. C. Smith, Holographic evaluation of warp in the torsion of a bar of cellular solid, Cellular Polymers, **14**, 1-13 (1995).

[35] Z. Rueger and R. S. Lakes, Experimental Cosserat elasticity in open cell polymer foam, under review.

[36] M. Brodt, L. S. Cook, and R. S. Lakes, Apparatus for determining the properties of materials over ten decades of frequency and time: refinements, Rev. Sci. Instrum. **66**, 5292-5297, 1995.

[37] T. Lee, R. S. Lakes, and A. Lal, Resonant ultrasound spectroscopy for measurement of mechanical damping: comparison with broadband viscoelastic spectroscopy, Rev. Sci. Instrum., **71**, 2855-2861, 2000.

[38] Y. C. Wang, R. S. Lakes, and Butenhoff, A., 2001, Influence of cell size on re-entrant transformation of negative Poisson's ratio reticulated polyurethane foams, Cellular Polymers, **20**, 373-385.

[39] J. B. Choi, R. S. Lakes, Nonlinear properties of polymer cellular materials with a negative Poisson's ratio, J. Materials Science, **27**, 4678-4684 (1992).

[40] D. Li, L. Dong, and R. S. Lakes, The properties of copper foams with negative Poisson's ratio via resonant ultrasound spectroscopy, Physica Status Solidi, **250**(10), 1983-1987 (2013).

[41] M. Bianchi, F. L. Scarpa, C. W. Smith, Stiffness and energy dissipation in polyurethane auxetic foams. Journal of Materials Science **43** (17), 5851-5860 (2008).

[42] J. N. Grima, D. Attard, R. Gatt and R. N. Cassar, A Novel Process for the Manufacture of Auxetic Foams and for Their re-Conversion to Conventional Form, Advanced Engineering Materials **11**, 533-535 (2009).

[43] A. A. Pozniak, J. Smardzewski, K. W. Wojciechowski, Computer simulations of auxetic foams in two dimensions, Smart Materials and Structures **22** (8) 084009 (11pp) (2013).

[44] A. Askar and A. S Cakmak, A structural model of a micropolar continuum, Int. J. Engng. Sci. **6**, 583-589, (1968).

[45] T. Tauchert, A lattice theory for representation of thermoelastic composite materials, Recent Advances in Engineering Science, **5**, 325-345 (1970).

[46] G. Adomeit, Determination of elastic constants of a structured material, Mechanics of Generalized Continua, (Edited by Kröner, E.), IUTAM Symposium, Freudenstadt, Stuttgart. Springer, Berlin (1967).

[47] A. Spadoni and M. Ruzzene, Elasto-static micropolar behavior of a chiral auxetic lattice, J. Mechs Physics of Solids, **60**, 156-171 (2012).

[48] R. S. Lakes and Drugan, W. J., Bending of a Cosserat elastic bar of square cross section - theory and experiment, J. Applied Mechanics, **82**(9), 091002 (2015)